Published in final edited form as:
NMR Biomed. 2013 December ; 26(12): 1768–1774. doi:10.1002/nbm.3016.

Effects of fat on MR-measured metabolite signal strengths: Implications for *in vivo* MR spectroscopy studies of the human brain

Anderson Mon, Ph.D.[1,2], **Christoph Abé, Dr. rer. nat.**[1], **Timothy C. Durazzo, Ph.D.**[1], and **Dieter J. Meyerhoff, Dr.rer.nat.**[1]

[1]Department of Radiology and Biomedical Imaging, University of California, San Francisco and Center for Imaging of Neurodegenerative Diseases, Veterans Administration Medical Center San Francisco, California, U.S.A

[2]Department of Biomedical Engineering, All Nations University College, Koforidua, Ghana

Abstract

Recent MRS studies indicate that higher body mass index (BMI) is associated with lower brain metabolite levels. Generally, individuals with higher BMIs have more body fat deposits than individuals with normal BMIs. This single voxel spectroscopy (SVS) study investigated possible effects of fat on MR-measured metabolite signal areas, which could partly explain the observed associations of BMI with MR-measured brain metabolite levels *in vivo*. SVS data were acquired at 4T from a phantom containing N-acetylaspartate (NAA), glutamate (Glu) and creatine as well as from three healthy male adults. Back fat obtained from the pig was used to assess the effects of fat on metabolite signals. With the same voxel size and placement, the phantom was first scanned without fat (baseline), then with 0.7 cm and 1.4 cm thick fat layers placed on it. Each participant was also scanned first without fat and then with two 0.7 cm fat layers: one placed beneath the occiput and the other on the forehead. Two spectra were acquired per participant from the anterior cingulate and the parieto-occipital cortices . The metabolite resonance and corresponding water peak areas were then fitted and metabolite-to-water signal ratios used for analyses. In both phantom and *in vivo* experiments, the metabolite-to-water ratios decreased in the presence of fat compared to baseline acquired in the absence of fat. The reduced metabolite signals in the presence of fat at 4T are reminiscent of the negative correlations observed between BMI and MR-measured metabolite levels. These apparent physical effects of fat have potentially far-reaching consequences for the accuracy of MR measurements of brain metabolite levels and their interpretation, particularly when large fat stores exist around the skull, such as in individuals with higher BMI.

Keywords

body mass index; MRS; metabolite concentration; body fat; rf absorption; dielectric effects

Address for correspondence: Dr. Anderson Mon, Department of Biomedical Engineering, All Nations University College, P. O. Box KF 1908, Koforidua, Eastern Region, Ghana, baarenaba@hotmail.com.

INTRODUCTION

Proton Magnetic Resonance Spectroscopy (1H MRS) is a noninvasive method of studying metabolite levels in the human brain. The metabolites routinely measured by 1H MRS at field strengths between 1.5 T and 4 T are N-acetylaspartate (NAA: a marker of neuronal integrity), glutamate (Glu: an excitatory neurotransmitter), creatine + phosphocreatine (Cr: a marker of mitochondrial energy metabolism), choline-containing compounds (Cho: a marker of glial or cell synthesis/turnover) and myo-inositol (mI: a putative astrocyte marker). The levels of these metabolites, derived from their corresponding peak areas in MR spectra, have been shown to change as a function of aging (Pfefferbaum et al., 1999b; Schuff et al., 1999b), neurodegenerative diseases (Pfefferbaum et al., 1999a; Valenzuala and Sachdev, 2001; Schuff et al., 1999c), various psychiatric disorders, (Ajilore et al., 2007; Bertolino et al., 1996; Bertolino et al., 1998; Hasler et al., 2007), as well as substance and /or alcohol use disorders (Abe et al., 2012; Durazzo et al., 2003; Durazzo et al., 2006; Meyerhoff and Durazzo, 2008; Mon et al., 2012a).

We recently observed that brain metabolite signal strengths are also influenced by body mass index (BMI, an index of adiposity), across different studies performed on 1.5T and 4T scanners, such that higher BMIs correspond to lower metabolite signals. Using 1.5T multi-slice MR spectroscopic imaging (MRSI), we reported negative correlations of BMI with NAA concentrations in frontal gray and white matter as well as parietal and temporal white matter of middle-aged healthy individuals (Gazdzinski et al., 2008). BMI also correlated negatively with frontal white matter Cho concentrations. Multi-slice MRSI data from the same MRI system also showed negative correlations of BMI with NAA, Cr, Cho and mI levels in the frontal lobe, subcortical nuclei and cerebellar vermis of middle-aged alcohol dependent individuals (Gazdzinski et al., 2010a). Further, 4T single voxel MRS of healthy elderly individuals also demonstrated lower NAA-to-Cr and NAA-to-Cho ratios in the anterior cingulate cortex in association with higher BMIs (Gazdzinski et al., 2010c). The similar findings at different magnetic field strengths using different pulse sequences suggest that BMI's effect on brain metabolite levels is independent of magnetic field strength or pulse sequence used. Our findings followed a similar report of lower glucose metabolism in the brain of healthy human individuals with higher BMIs (Volkow et al., 2008), suggesting that our findings of a BMI-metabolite concentration association had a biological rather than purely methodological/technical basis. Taken together, the negative association of BMI with brain metabolite levels was interpreted as BMI-related neuronal and/or myelin abnormalities particularly in the frontal regions (Gazdzinski et al., 2008), and that higher BMIs may be associated with accelerated aging and increased odds of developing age-related diseases, such as mild cognitive impairment and Alzheimer's disease.

In a recent report using 3T MRSI, Maudsley and colleagues suggested that the negative associations between BMI and brain signal integrals could be partly due to physical reasons (Maudsley et al., 2012). This is because they observed that higher BMIs were associated with broader spectral line widths, particularly in spectra from frontal and parietal brain regions. Also, higher BMIs were generally associated with decreased signal to noise ratios and increased uncertainties of spectral fitting (observed with the Cramer-Rao lower bounds of NAA spectral fits). The authors therefore argued that the poorer spectral line shapes

arising from these factors could lead to poorer baseline fitting of spectra and a corresponding underestimation of metabolite signals from individuals with higher BMIs, which could at least partly explain the observed correlations of BMI with MRS metabolite signals. In this report, we aimed to test this view by Maudsley et al. by assessing effects of fat placed close to a spectroscopy voxel, and we suggest that other physical factors can also contribute to the lower MR-measured metabolite levels in individuals with higher BMIs. For instance, at magnetic fields such as 3T or 4T, field-focusing (which makes the rf field at the origin much stronger than further out in the sample (Hoult, 2000)) and dielectric effects introduce spatially varying non-uniform B_1 fields. Regions of lower B_1 experience smaller excitation flip angles, which would affect metabolite signals equally across the metabolite chemical shift range (including the co-localized water peaks), but may be more pronounced in individuals with higher BMI. Another physical phenomenon that could be playing a part is rf absorption by fat. Since fat content varies with BMI, the amount of radiation absorbed will be BMI dependent. In this context, the more head fat encountered by the rf field (a scenario in higher BMI individuals), the greater the rf energy absorption and the smaller the MR signal received .

In this study we investigated effects of fat on observed MRS metabolite levels using single voxel spectroscopy (SVS) on a 4T MR scanner. Specifically, we tested the hypothesis that metabolite levels observed by SVS 1H MRS are lower when fat is in the vicinity of the region of interest.

Method

Materials and MRS acquisition methods

We conducted SVS experiments on a phantom and on three healthy human volunteers. The phantom consisted of a saline-filled cylindrical plastic bottle (diameter = 11.5cm, height = 20cm) containing a smaller cylindrical plastic bottle (diameter = 5.5cm, height = 10cm) that contained 100mM of NAA, Glu and Cr each in a buffered solution (pH = 7.2). The three healthy male volunteers were 30, 31 and 55 years old, with BMI of 25.9 kg/m^2, 23.5 kg/m^2 and 25.6 kg/m^2 respectively. They all signed a formal written consent form approved by the committee on human research of the University of California San Francisco. Pig fat was purchased from a local butcher and sliced into rectangular sheets of 0.7 cm thick. The fat sheets were attached to the phantom or placed on the forehead and occiput of the participants to assess the postulated effects of fat on MR-measured metabolite signals.

All SVS data were acquired on a 4T Bruker MedSpec scanner with Siemens Trio software and a transmit and receive head coil (8-channels). First, three dimensional (3D) sagittal T1-weighted and 2D axial T2-weighted anatomical images were acquired with a Magnetization Prepared Rapid Gradient Echo sequence (TR/TE/TI = 2300/3/950 ms, 7° flip angle, 1.0 × 1.0 × 1.0 mm^3 resolution) and a spin-echo sequence (TR/TE = 8400/70 ms, 150° flip angle, 0.9 × 0.9 × 3 mm^3 resolution), respectively. Both anatomical images were then displayed and used for volumes-of-interest (VOIs) placement. After 3D shimming and water suppression before each experiment (first without fat, then with fat), metabolite signals were acquired with a Stimulated Echo Acquisition Mode (STEAM) sequence (TR/TE/TM = 2000/12/10 ms, 90° flip angle, 2000 Hz spectral bandwidth, 2.5 minutes acquisition time).

Immediately afterwards, a reference water signal was acquired from the same VOIs with the same STEAM sequence, but without water suppression; the water signal was used to normalize the metabolite peak areas. The transmitter voltage amplitude was adjusted in each SVS experiment to give a 90° excitation pulse in the VOI, but the receiver gain was kept constant across experiments. The transmitter reference voltages for a 90 degree flip angle were similar in baseline and fat experiments.

Experiments

Phantom—Three experiments were performed on the phantom: without fat (baseline data), with one layer of fat (7 mm × 90 mm × 130 mm slab) and with two layers of fat (2 * 7 mm × 90 mm × 130 mm slab) placed on the phantom. A fixed VOI size of dimensions 35×25×20 mm^3 and a location with the closest edge being about 15 mm away from the fat layer was used in all phantom experiments. At this position of the VOI, MRS signal contamination from the fat was negligible.

In Vivo—Each of the three participants was scanned twice: first without fat (baseline data), then with one layer of fat (7 mm × 35 mm × 43 mm slab) placed underneath the occiput and a similar layer placed on the forehead (see top row of Figure 1). In each experiment SVS data were acquired from two VOIs: one of size 35 × 25 × 20 mm^3 in the anterior cingulate (ACC) and the other of size 40 × 20 × 20 mm^3 in the parieto-occipital cortex (POC). The bottom row of Figure 1 shows the two VOIs on axial T2-weighted images. To minimize head motion due to long scan time participants were given a 10-minute break between the scans. Also fast localizers were acquired before and after each VOI acquisition to check for movement; no significant movement was detected in any *in vivo* experiment.

Data Processing

We used two different methods to extract metabolite peak areas from the phantom experiments. To rule out the possibility of baseline fitting inaccuracies resulting in metabolite signal reductions, we first estimated the spectral peak areas manually to avoid baseline fitting. We assumed that the spectral peak shapes were Gaussian and applied the formula $A = I*FWHM / 0.9374$ to estimate the singlet peak areas of NAA at 2.02 ppm and Cr at 3.03 ppm (A is peak area, I is the amplitude of the peak and FWHM is the full width at half maximum of the peak). We estimated the uncertainty of the spectral peak area measures by taking the read-off accuracies of the processing software scales (1 unit for amplitude; 0.003ppm (0.5 Hz) for FWHM) into account. Because of the J-coupled resonances of the Glu peak, we could not presume its shape; therefore we did not estimate Glu area with this method. In the second method, we fitted the data (metabolites and water) using IDL (Research Systems, Inc., Boulder, CO) with SITOOLS (see (Soher et al., 1998)). We did not fit the baseline in the phantom data (since no significant baseline rolls were present), thereby avoiding the potential effects of baseline fitting inaccuracies.

The *in vivo* SVS data were also fitted with the same software as the phantom data, but with baseline fitting enabled, the method employed in all our quantitative MRS analyses (Gazdzinski et al., 2008; Gazdzinski et al., 2010a; Gazdzinski et al., 2010b). Using *a priori* information of metabolite frequencies, line widths, and amplitudes, spectral peak areas for

NAA, Glu, Cr, Cho and mI as well as the corresponding unsuppressed H_2O peak area were fitted. The bottom spectrum of Figure 2 shows a typical spectral fit that was considered a good fit.

All metabolite peak areas (in both phantom and *in vivo* experiments) were then scaled to the corresponding H_2O peak area to account for the effects of differences in transmitter voltage for a 90 degree pulse (if any), coil sensitivity changes and other unknown factors that would affect metabolite signals equally across experiments.

Results

Phantom experiments

Figure 3B and C show plots of the NAA/H_2O, Glu/H_2O and Cr/H_2O ratios for the three experiments. Only slight line broadening was observed across experiments in which fat was used (as can be seen in Figure 3A). The FWHMs of all metabolite as well as reference water spectra increased similarly by 0.25 Hz upon the placement of each fat layer. This broadening was less than the read-off accuracy of 0.50 Hz. Nevertheless, the ratios of the metabolites-to-water decreased in the presence of fat and with increasing fat thickness. Based on the metabolite area estimations using the Gaussian formula, NAA/H_2O decreased by 18% and Cr/H_2O by 9% (on average) between the baseline and the 0.7 cm thick fat layer experiments. NAA/H_2O further decreased by 10% and Cr/H_2O by 7% when the second fat layer was added. On average, the overall signal decrease from baseline to the setup with two fat layers was 26% for NAA/H_2O and 15% for Cr/H_2O. These decreases were greater than our estimated error of 10%. A similar pattern of results was obtained when metabolite and reference water peak areas were obtained with software fitting (Figure 3c): NAA/H_2O decreased by 26% and Cr/H_2O by 34% from baseline to the setup with two fat layers. Glu/H_2O, which was not estimated with the Gaussian formula, also decreased by 21% from baseline to the setup with two fat layers.

In vivo experiments

In the ACC, the FWHM of the *in vivo* spectra were about 0.8 Hz broader in the experiments with fat than in the baseline experiments (spectra not shown here). However, in the POC, no spectral broadening was observed in the presence of fat (Figure 4a). Figure 4b and c show plots of NAA/H_2O, Glu/H_2O, Cr/H_2O and Cho/H_2O ratios for experiments without and with fat in ACC and POC, respectively, for one participant. Plots of the metabolite-to-water ratios for the other participants showed similar patterns. Averaged across the three volunteers and in the ACC, NAA/H_2O decreased by 22%, Glu/H_2O by 21%, Cr/H_2O by 18% and Cho/H_2O by 16% in the presence of fat and relative to the average baseline ratios. In the POC, the corresponding average reductions were 20%, 14%, 16% and 12%. Table 1 and 2 show for both VOIs studied the metabolite ratios for both experiments, mean values of ratios (calculated across the three participants for baseline and fat experiments separately) and percentage change of the ratios in the presence of fat for all three participants individually. Apart from the fact that metabolite ratios consistently decreased in the presence of fat, the magnitude of the decreases were greater than methodological error, which was about 5% as calculated from test-retest data of 10 middle-aged healthy controls studied seven months

apart on the same magnet and with similar VOI positions (data not shown here). Metabolic changes over that time period are deemed negligible, and, indeed, the metabolite-to-water ratio changes for individual participants over the 7-months interval showed increases as well as decreases; i.e., no consistent directionality.

The non-normalized metabolite peak areas also showed a pattern of decrease in the presence of fat in both phantom and *in vivo* experiments similar to the pattern presented here for metabolite-to-water ratios. However, the reference water peak areas did not change appreciably and consistently in the presence of fat in either phantom or *in vivo* experiments (data not shown), suggesting a frequency dependent effect.

DISCUSSION

The aim of this study was to assess the degree to which fat in the vicinity of a spectroscopy VOI may have an effect on spectral signal intensities. The levels of NAA, Glu, Cr and Cho were studied using a phantom and three healthy volunteers as a proof of concept. With the phantom experiments we observed that the spectral peak areas of NAA, Glu and Cr and their ratios to co-localized H_2O decreased in the presence of externally added fat and further decreased with increasing the thickness of the fat layer. Similar reductions in metabolite area ratios, with some small spectral line broadening, were observed in the *in vivo* studies: NAA/H_2O, Glu/H_2O, Cr/H_2O and Cho/H_2O all decreased when adding an external fat layer to the head. Generally, the metabolite signal intensities were affected non-linearly (as seen in the phantom experiments), and appeared to be affected to slightly different extents by the presence of fat, with NAA affected most and Cho least.

The reductions in metabolite ratios of both phantom and *in vivo* studies in the presence of fat confirm our hypothesis that fat has an effect on MR-measured metabolite signals in a given spectroscopy voxel. Maudsley and colleagues (2012) observed associations of BMI with spectral line widths, SNR, macroscopic susceptibility profiles and spectral fitting uncertainties in some of the regions of the brain where BMI was significantly associated with metabolite values. The authors therefore suggested that the negative associations of BMI with MR-measured metabolite levels may be due to spectral fitting inaccuracies, which become more pronounced with broader spectral line-widths in individuals with higher BMI. Although we also observed some slight line-broadening in spectra from the phantom and ACC as a result of adding external fat in this study, we did not observe such line broadenings in POC spectra in the presence of fat, yet we found significant decreases of metabolite ratios similar to those observed in the ACC. Also, metabolite peak areas obtained from the high signal-to-noise phantom spectra, void of baseline fitting inaccuracies, decreased in the presence of fat, showing that line-width broadening and potentially associated baseline fitting inaccuracies did not contribute substantially to the smaller MR-measured metabolite signals observed in the presence of added fat.

In MR experiments, factors such as coil loading, coil sensitivity, rf field-focusing and dielectric effects can affect signal intensity. When coil loading approaches extreme values and a 90° excitation angle is not achieved due to limited rf power, weaker overall MR signal can be observed. However, this factor could not have reasonably affected the MR signals in

our experiments, because we did not observe a clear pattern of transmitter voltage increases (an indication of increase in coil loading) in the presence of fat and at constant receiver gain. Also Coil sensitivity effects due to fat could not have contributed substantially to the reductions in the metabolite signals since our reported measures are metabolite-to-water ratios, which, at least partially, accounted for coil sensitivity effects. Furthermore, rf field-focusing (Hoult, 2000) depends on only the strength of the main magnetic field but not on the sample nature or size; and therefore cannot be attributable tothe fat-associated smaller metabolite signals observed in this report. At 4 T, dielectric effects can affect signal intensities, since the wavelength (18 cm) of the rf field is similar to the dimensions of the human head (see Lee et al., 2002). These effects may be more pronounced with larger heads that have dimensions equal to/or greater than 18 cm (presumed to be the case in larger individuals with higher BMI or when placing a layer of fat on the human head) than heads that have dimensions less than 18 cm. However, since the associations of the metabolite signals with BMI are also observed at 1.5 T (Gazdzinski et al., 2008; Gazdzinski et al., 2010a) and 3 T (Maudsley et al., 2012), dielectric effects do not seem to be a major cause of the observed associations between metabolites and fat observed here, because such dielectric effects on the human head would not be expected at field strengths lower than 4 T. Additionally, dielectric effects would affect metabolite and reference water peak areas in the same manner, so that metabolite-to-water ratios should not be affected.

One physical phenomenon that can contribute significantly to the decrease in the metabolite signals in the presence of fat is absorption of the rf radiation. For instance, when an electromagnetic (EM) radiation is applied to a medium, molecules (or atoms) in the medium interact with the radiation. This interaction can lead to absorption of some power of the radiation by the medium (see (Baker-Jarvis and Kim, 2012)). Thus, the power of the radiation exiting the medium is reduced compared to that of the source radiation. In this context, fat could absorb and reduce the power of the excitation radiation as well as the emitted signal from the target VOI before detection by the receiver. In this way, the more surrounding fat there is, the greater the absorption and the lower the corresponding received signal, just as we observed in the phantom experiments. Consistent with this interpretation, Sandrini and colleagues reported higher specific absorption rate of EM energy (in the radio frequency range) in women than in men, mainly because of a thicker subcutaneous fat layer in women (Sandrini et al., 2004).

Also, the apparent exponentially decaying nature of the metabolites signals with fat thickness in the phantom experiments of this study (as seen in Figure 3b and c) suggests the presence of a substantial absorption component in the overall metabolite signal drop due to the presence of fat. This is because the Lambert-Bouguer law states that attenuation of radiation varies exponentially with the thickness of the absorbing medium it passes through. However, experiments using several different fat layers are needed to confirm the exponential nature of the metabolite ratios-to-fat thickness observed here with only three data points. It is also important to note that these potential absorption effects observed appear to be frequency dependent, since the extent of the metabolite signal reduction depended on chemical shift, with NAA experiencing the highest reduction and Cho the lowest.

The associations of fat with MR-measured metabolite signals in the experiments described here suggest that the inverse relation between BMI and *in vivo* MR-measured brain metabolite levels may be strongly modulated by the presence of fat in the vicinity of the VOI, i.e., fat surrounding the brain. This is because individuals with higher BMI can reasonably be expected to have more fat deposits on the head than individuals with lower BMI. Consistent with this explanation, Verstynen et al. reported that MR diffusion tensor imaging signals were weaker in individuals with higher BMI than in those with normal BMI (Verstynen et al., 2012).

The findings of the current study therefore highlight the need for careful interpretation of any associations of BMI or other body fat measures with MR-based outcome measures, as these measures may be affected by surrounding body fat. On this note, our previous findings of inverse relations between BMI and MRS-measured brain metabolite signals may be confounded by the effects of surrounding fat.

Despite these new observations, it is entirely possible that biological reasons also contribute to the observed associations of BMI with MRS-measured metabolite levels. However, this can only be demonstrated unequivocally by studies that account for the apparent non-linear physical effects of fat reported here. With far greater relevance to all clinical MRS studies, our findings suggest a need to account for fat effects when analyzing MRS-measured brain metabolite data, and possibly other MR measures such as brain volumes, densities, or water diffusion. Covarying MR signal measures for BMI, as done sometimes, may not appropriately account for the effects of fat, since BMI and the amount of fat on the head may not necessarily correlate strongly. An effective fat correction factor may be composed by measurement of fat content and distribution surrounding an individual’s head, but this complex problem requires careful studies. In the mean time, software tools exist that quantitate the fat surrounding the brain on suitable brain images, which then could be used as a proxy measure of the fat surrounding an individual’s head. While this is not ideal (the location of fat with respect to the VOI may play a critical role), it may be better than simply using BMI as a proxy.

As in every study, this report has its limitations. The phantom used in this study did not contain Cho and mI, which are some of the metabolites that we reported to be associated with BMI. Therefore, we could not determine the experimental behavior of these metabolite signals in the presence of fat. In the *in vivo* experiments the effects of fat on Cho signal were assessed; however, we did not fit mI because of the generally poorer spectral fits around the mI peak due to the nature and extent of residual water signal. Also, the sample size of the human participants was very small, thus rigorous statistical analyses to assess significant differences between metabolite data of experiments without fat and those with fat could not be carried out. Furthermore we did not specifically measure coil loading to assess its effects on the experiments without fat and with fat; we only used changes in optimized transmitter voltage to show that there were no unidirectional or significant changes in coil loading. Finally, we did not perform our experiments on different MRI systems or at different field strengths; and we did not test these effects of fat on metabolite signals using the widely used PRESS sequence . Therefore, morefollow-up studies are needed to support and further clarify the circumstances under which metabolite signal is affected by nearby fat.

Assessments of the dependence of fat effects on rf coil type and on the distance between coil and fat as well as fat and VOI are also warranted. Notwithstanding these limitations, our findings reveal easily measurable effects of fat on MRS-measured metabolite signals at 4 T, which, to the best of our knowledge, have not been described previously at any field strength. This work adds new information to our understanding of the limitations of *in vivo* brain 1H MRS.

In conclusion, we demonstrated that fat in the vicinity of an MR spectroscopy volume reduces 1H MRS-measured metabolite signals non-linearly at 4 T, and we discuss several factors that can affect metabolite signals, including rf absorption as the most likely source of our findings. Because of this fat-related signal reduction, the biological relevance of associations of BMI with MRS-measured brain metabolites levels should be interpreted with caution: such associations may be confounded by the amount of fat surrounding the brain, therefore linking these associations to a physical in addition to any possible biological phenomenon. The existence of these physical effects may have far-reaching consequences for the accuracy of both absolute and relative *in vivo* metabolite concentration measurements and their interpretation, in particular when large fat stores exist around the skull, such as in individuals with higher BMI.

Acknowledgments

The authors are very grateful to Drs. Gerald Matson and Norbert Schuff for their valuable intellectual contributions to this work. This work was supported by the National Institutes of Health AA10788 (DJM), DA025202 (DJM) and resources and facilities at the San Francisco Veterans Administration Medical Center. The authors have no disclosures or conflicts of interest to report.

List of Abreviations

ACC	anterior cingulate
BMI	body mass index
Cr	creatine
Cho	choline containing compounds
D	dimensional
EM	electromagnetic
FWHM	full wave at half maximum
Glu	glutamate
H	proton
H_2O	water
mI	myo-inositol
MR	magnetic resonance
MRI	magnetic resonance imaging
MRS	magnetic resonance spectroscopy

MRSI	magnetic resonance spectroscopic imaging
NAA	n-acetyl aspartate
POC	parietal-occipital cortex
PRESS	point resolved spectroscopy
SNR	signal-to-noise ratio
STEAM	stimulated echo acquisition mode
T	Tesla
TE	echo time
TI	inversion time
TM	mixing time
TR	repetition time
VOI	voxel of interest.

References

Abe C, Mon A, Durazzo TC, Pennington DL, Schmidt TP, Meyerhoff DJ. Polysubstance and alcohol dependence: Unique abnormalities of magnetic resonance-derived brain metabolite levels. Drug Alcohol Depend. 2012

Ajilore O, Haroon E, Kumaran S, Darwin C, Binesh N, Mintz J, Miller J, Thomas MA, Kumar A. Measurement of brain metabolites in patients with type 2 diabetes and major depression using proton magnetic resonance spectroscopy. Neuropsychopharmacology. 2007; 32:1224–1231. [PubMed: 17180124]

Baker-Jarvis J, Kim S. The Interaction of Radio-Frequency Fields with Dielectric Materials at Macroscopic to Mesoscopic Scales. Journal of Research of the National Institute of Standards and Technology. 2012; 117:1–60.

Bertolino A, Nawroz S, Mattay VS, Barnett AS, Duyn JH, Moonen CT, Frank JA, Tedeschi G, Weinberger DR. Regionally specific pattern of neurochemical pathology in schizophrenia as assessed by multislice proton magnetic resonance spectroscopic imaging. Am J Psychiatry. 1996; 153:1554–1563. [PubMed: 8942451]

Bertolino A, Callicott JH, Nawroz S, Mattay VS, Duyn JH, Tedeschi G, Frank JA, Weinberger DR. Reproducibility of proton magnetic resonance spectroscopic imaging in patients with schizophrenia. Neuropsychopharmacology. 1998; 18:1–9. [PubMed: 9408913]

Durazzo TC, Gazdzinski S, Meyerhoff DJ. Brain metabolite concentrations and cognition during short-term abstinence from alcohol. Alcohol Clin Exp Res. 2003; 27:21A.

Durazzo TC, Gazdzinski S, Banys P, Meyerhoff DJ. Brain metabolite concentrations and neurocognition during short-term recovery from alcohol dependence: Preliminary evidence of the effects of concurrent chronic cigarette smoking. Alc Clin Exp Research. 2006; 30:539–551.

Elias MF, Elias PK, Sullivan LM, Wolf PA, D'Agostino RB. Lower cognitive function in the presence of obesity and hypertension: the Framingham heart study. Int J Obes Relat Metab Disord. 2003; 27:260–268. [PubMed: 12587008]

Gazdzinski S, Kornak J, Weiner MW, Meyerhoff DJ. Body mass index and magnetic resonance markers of brain integrity in adults. Ann Neurol. 2008; 63:652–657. [PubMed: 18409192]

Gazdzinski S, Durazzo TC, Mon A, Meyerhoff DJ. Body mass index is associated with brain metabolite levels in alcohol dependence--a multimodal magnetic resonance study. Alcohol Clin Exp Res. 2010a; 34:2089–2096. [PubMed: 21087290]

Gazdzinski S, Durazzo TC, Mon A, Meyerhoff DJ. Body Mass Index Is Associated With Brain Injury In Alcohol Dependence - A Multimodal Magnetic Resonance Study. Alc Clin Exp Research. 2010b (in press).

Gazdzinski S, Millin R, Kaiser LG, Durazzo TC, Mueller SG, Weiner MW, Meyerhoff DJ. BMI and neuronal integrity in healthy, cognitively normal elderly: a proton magnetic resonance spectroscopy study. Obesity (Silver Spring). 2010c; 18:743–748. [PubMed: 19816410]

Gunstad J, Paul RH, Cohen RA, Tate DF, Spitznagel MB, Gordon E. Elevated body mass index is associated with executive dysfunction in otherwise healthy adults. Compr Psychiatry. 2007; 48:57–61. [PubMed: 17145283]

Hasler G, van der Veen JW, Tumonis T, Meyers N, Shen J, Drevets WC. Reduced prefrontal glutamate/glutamine and gamma-aminobutyric acid levels in major depression determined using proton magnetic resonance spectroscopy. Arch Gen Psychiatry. 2007; 64:193–200. [PubMed: 17283286]

Hoult DI. Sensitivity and Power Deposition in a High-Field Imaging Experiment. J. Magn. Reson. Imaging. 2000; 12:46–67. [PubMed: 10931564]

Lee A, Choi H, Lee H, Pack J. Human Head Size and SAR Characteristics for Handset Exposure. ETRI Journal. 2002; 24:176–180.

Maudsley AA, Govind V, Arheart KL. Associations of age, gender and body mass with 1H MR-observed brain metabolites and tissue distributions. NMR Biomed. 2012; 25:580–593. [PubMed: 21858879]

Meyerhoff DJ, Durazzo TC. Proton magnetic resonance spectroscopy in alcohol use disorders: a potential new endophenotype? Alcohol Clin Exp Res. 2008; 32:1146–1158. [PubMed: 18540913]

Mon A, Durazzo T, Meyerhoff DJ. Glutamate, GABA, and Other Cortical Metabolite Concentrations during Early Abstinence from Alcohol and their Associations with Neurocognitive Changes. Drug & Alcohol Dependence. 2012a; 125:27–36. [PubMed: 22503310]

Mon A, Durazzo TC, Gazdzinski S, Hutchison KE, Pennington D, Meyerhoff DJ. Brain-derived Neurotrophic Factor (BDNF) Genotype is Associated with Lobar Gray and White Matter Volume Recovery in Abstinent Alcohol Dependent Individuals. Genes Brain Behav. 2012b

Pfefferbaum A, Adalsteinsson E, Spielman D, Sullivan EV, Lim KO. In vivo brain concentrations of N-acetyl compounds, creatine, and choline in Alzheimer disease. Archives of General Psychiatry. 1999a; 56:185–192. [PubMed: 10025444]

Pfefferbaum A, Adalsteinsson E, Spielman D, Sullivan EV, Lim KO. In vivo spectroscopic quantification of the N-acetyl moiety, creatine, and choline from large volumes of brain gray and white matter: effects of normal aging. Magnetic Resonance in Medicine. 1999b; 41:276–284. [PubMed: 10080274]

Sandrini L, Vaccari A, Malacarne C, Cristoforetti L, Pontalti R. RF dosimetry: a comparison between power absorption of female and male numerical models from 0.1 to 4 ghz. Phys Med Biol. 2004; 49:5185–5201. [PubMed: 15609567]

Schuff N, Amend D, Knowlton R, Tanabe J, Norman D, Fein G, Weiner MW. Age-related metabolite changes and volume loss in hippocampus by proton MR spectroscopic imaging and MRI neurobiology of aging. Neurobiology of Aging. 1999b; 20:279–285. [PubMed: 10588575]

Schuff N, Vermathen P, Maudsley AA, Weiner MW. Proton magnetic resonance spectroscopic imaging in neurodegenerative diseases. Current Science. 1999c; 76:800–807.

Soher BJ, Young K, Govindaraju V, Maudsley AA. Automated spectral analysis III: application to in vivo proton MR spectroscopy and spectroscopic imaging. Magn Reson Med. 1998; 40:822–831. [PubMed: 9840826]

Stanek KM, Grieve SM, Brickman AM, Korgaonkar MS, Paul RH, Cohen RA, Gunstad JJ. Obesity is associated with reduced white matter integrity in otherwise healthy adults. Obesity (Silver Spring). 2011; 19:500–504. [PubMed: 21183934]

Valenzuala MJ, Sachdev P. Magnetic Resonance Spectroscopy in AD. Neurology. 2001; 56:592–598. [PubMed: 11261442]

Verstynen TD, Weinstein AM, Schneider WW, Jakicic JM, Rofey DL, Erickson KI. Increased body mass index is associated with a global and distributed decrease in white matter microstructural integrity. Psychosom Med. 2012; 74:682–690. [PubMed: 22879428]

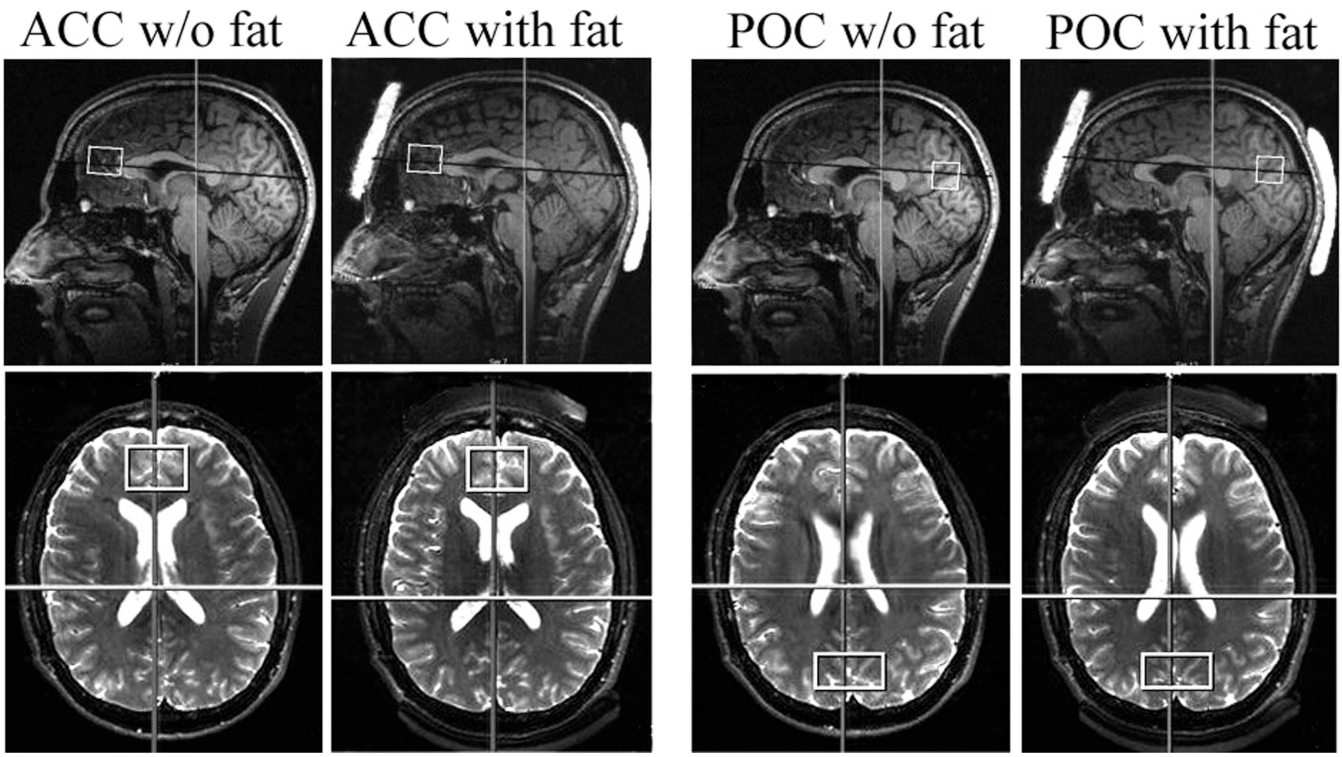

Figure 1.

Sagittal T1-weighted (top) and axial T2-weighted (bottom) images showing the positions of the fat layers on the head and the VOIs in the brain from one *in vivo* experiment. Left panel: ACC (with and without fat layers), Right panel: POC (with and without fat layers).

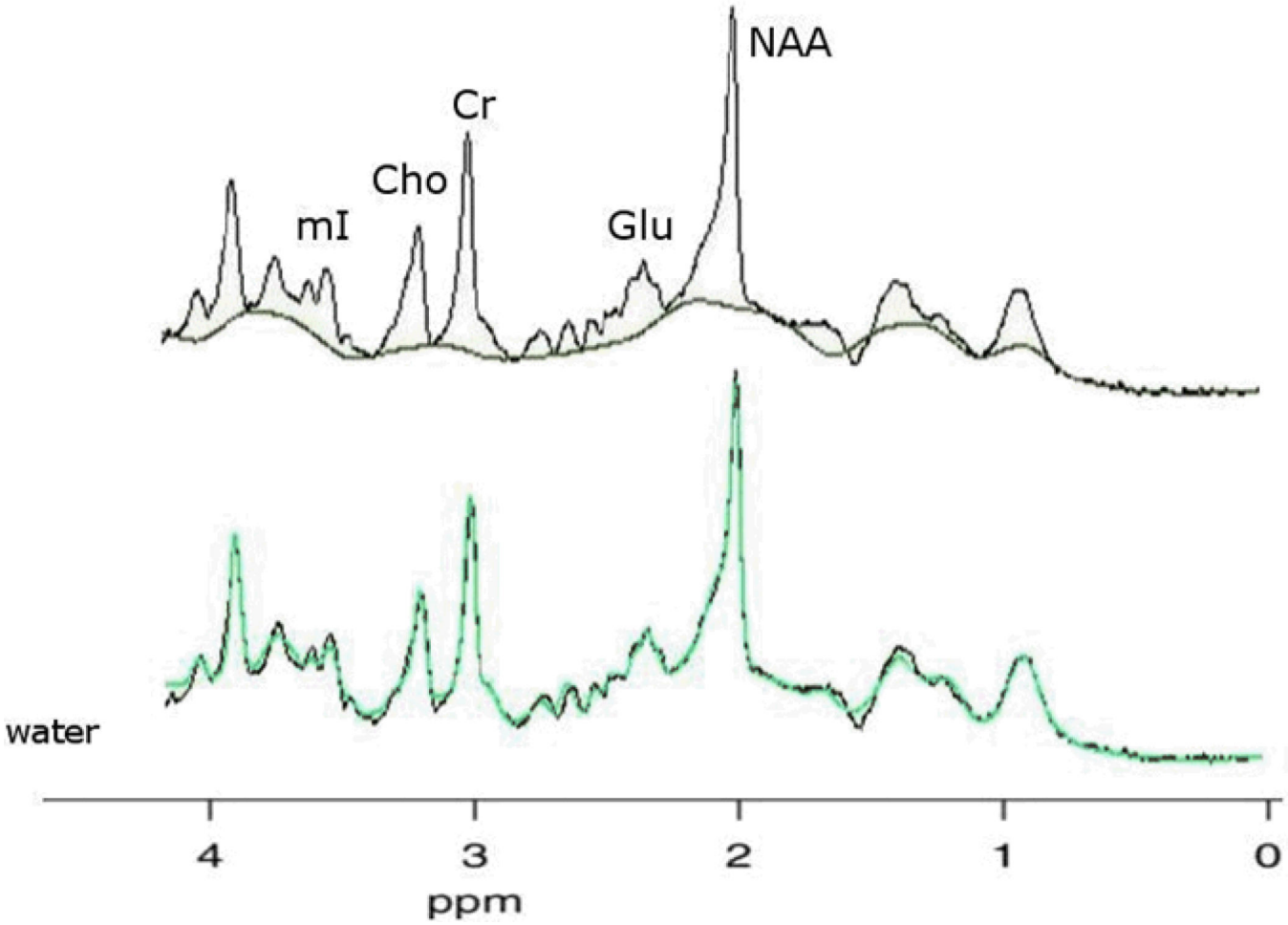

Figure 2.

In vivo spectra of human brain fitted with the SITOOLS software. Top spectrum illustrates a typical good baseline fit between 1.8 and 4.2 ppm. Any peak areas above the baseline are fit by the spectral model, including macromolecules. The bottom spectrum illustrates a typical good model fit. The black line represents the acquired data, the green line the sum of spectral and baseline model used.

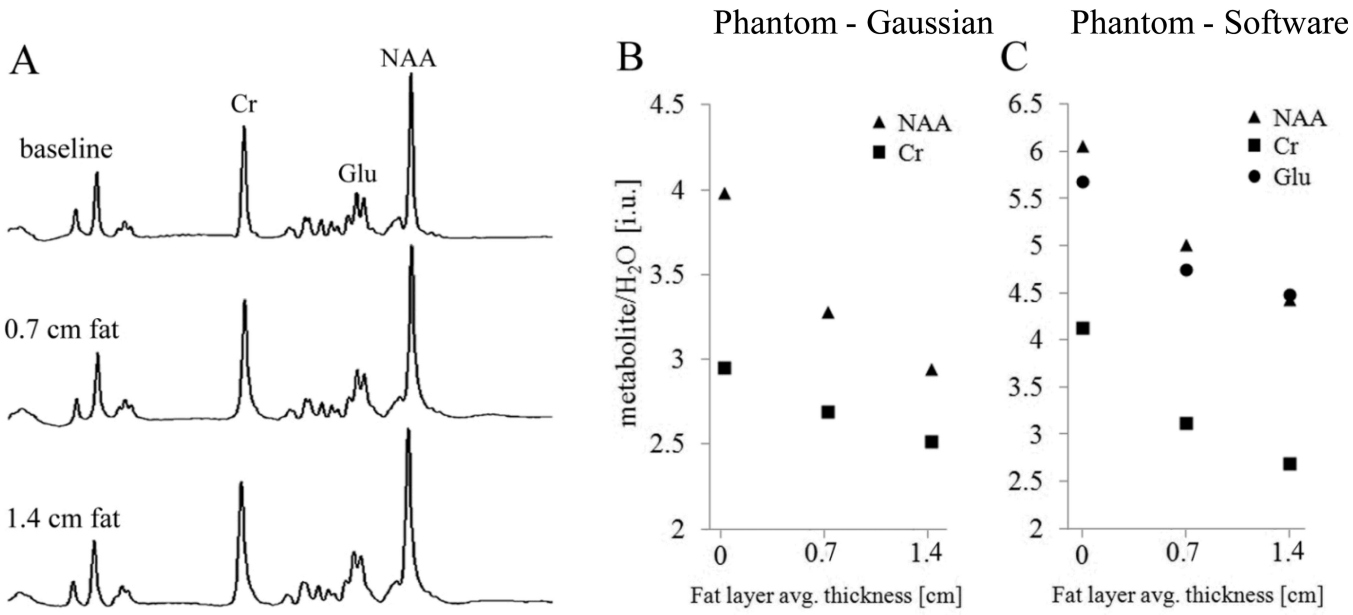

Figure 3.

NAA, Glu and Cr spectra of phantom (**panel A**: spectra are not on the same vertical scale) and plots of metabolite/H_2O ratios from acquired data against fat thickness. **Panel B**: NAA/H_2O and CR/H_2O ratios estimated using Gaussian formula; **panel C**: NAA/H_2O, Glu/H_2O and CR/H_2O ratios obtained from software fitting. Notice the slight spectral line broadening of the middle and bottom spectra acquired in the presence of fat when compared with the top spectrum (baseline).

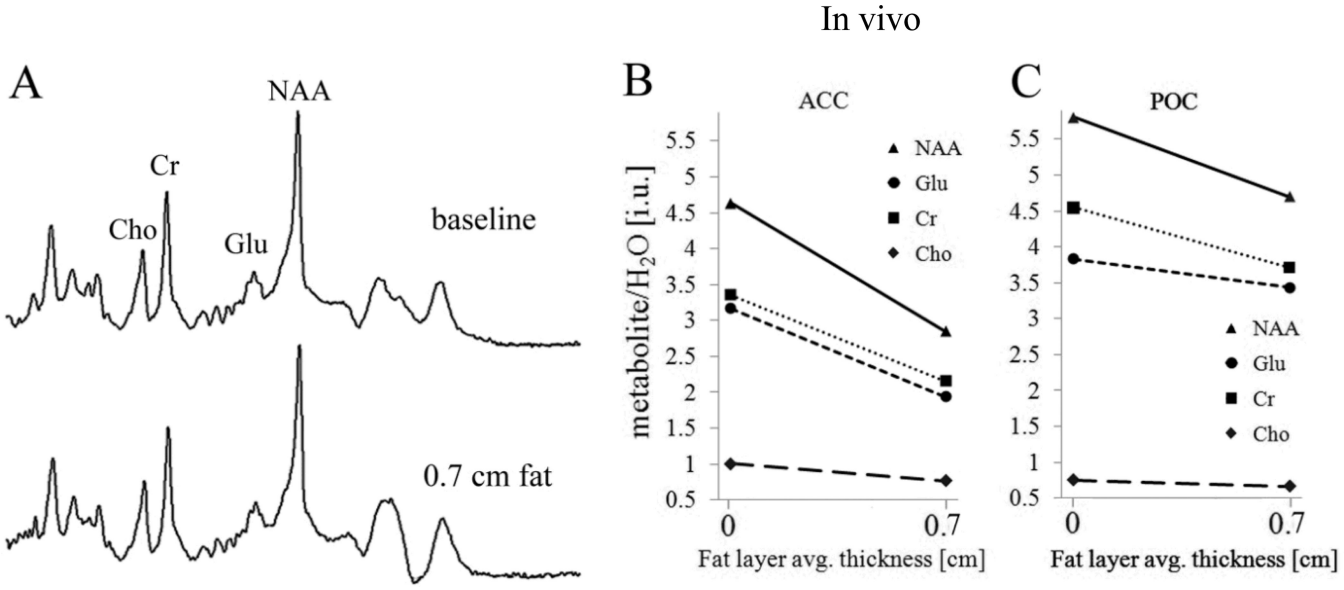

Figure 4.

In vivo brain metabolite spectra for the POC voxel (**panel A**: spectra are not on the same vertical scale). Plots of NAA/H_2O, Glu/ H_2O, CR/H_2O and Cho/H_2O ratios against fat thickness for one participant in ACC (**Panel B**) and POC (**Panel C**). (Note: In **Panel B**, the values for ACC Glu/H_2O and Cr/H_2O were very similar in one of the participants (participant 2), but for the purpose of clarity, they are shown separated by decreasing the Glu/ H_2O values slightly.

Table 1

ACC metabolite-to-water ratios (for all participants) together with their means and standard deviations across participants for baseline and fat experiments

Metabolite	Participant 1			Participant 2			Participant 3			Mean ± standard deviation across Participants	
	W/o fat	*With fat*	*%diff*	*W/o fat*	*With fat*	*%diff*	*W/o fat*	*With fat*	*%diff*	*W/o fat*	*With fat*
NAA/H_2O	3.93	3.35	−15	4.63	2.85	−37	4.00	3.40	−15	4.19 ± 0.39	3.20 ± 0.30
Glu/H_2O	3.06	2.72	−11	3.37	2.14	−36	3.12	2.61	−16	3.18 ± 0.16	2.49 ± 0.31
Cr/ H_2O	3.21	2.70	−15	3.36	2.15	−36	2.91	2.79	−4	3.16 ± 0.23	2.55 ± 0.35
Cho/ H_2O	0.84	0.76	−10	1.00	0.77	−23	0.83	0.71	−14	0.89 ± 0.10	0.75 ± 0.03

Table 2

POC metabolite-to-water ratios (for all participants) together with their means and standard deviations across participants for baseline and fat experiments

Metabolite	Participant 1			Participant 2			Participant 3			Mean ± standard deviation across Participants	
	W/o fat	*With fat*	*%diff*	*W/o fat*	*With fat*	*%diff*	*W/o fat*	*With fat*	*%diff*	*W/o fat*	*With fat*
NAA/H_2O	4.87	3.86	−21	5.80	4.70	−19	5.21	4.25	−19	5.29 ± 0.47	4.27 ± 0.42
Glu/H_2O	3.34	2.87	−14	3.83	3.4	−10	4.21	3.46	−18	3.79 ± 0.44	3.24 ± 0.32
Cr/ H_2O	3.87	3.26	−16	4.55	3.71	−18	4.20	3.60	−14	4.21 ± 0.34	3.52 ± 0.23